

# Innovative Design and Simulation of a Transformable Robot with Flexibility and Versatility, RHex-T3

Yue Lin<sup>1</sup>, Yujia Tian<sup>1</sup>, Yongjiang Xue<sup>1</sup>, Shujun Han<sup>1</sup>, Huaiyu Zhang<sup>1</sup>,  
Wenxin Lai<sup>1</sup> and Xuan Xiao<sup>1</sup>

**Abstract**—This paper presents a transformable RHex-inspired robot, RHex-T3, with high energy efficiency, excellent flexibility and versatility. By using the innovative 2-DoF transformable structure, RHex-T3 inherits most of RHex's mobility, and can also switch to other 4 modes for handling various missions. The wheel-mode improves the efficiency of RHex-T3, and the leg-mode helps to generate a smooth locomotion when RHex-T3 is overcoming obstacles. In addition, RHex-T3 can switch to the claw-mode for transportation missions, and even climb ladders by using the hook-mode. The simulation model is conducted based on the mechanical structure, and thus the properties in different modes are verified and analyzed through numerical simulations.

## I. INTRODUCTION

In recent decades, more and more researchers involve in the study of mobile robots to overcome various environments. RHex is undoubtedly one of the most successful mobile robots in terms of flexibility [1][2]. With the simple mechanical structures and only 6 actuators, RHex performs the incredible mobility at the cost of low energy consumption[3][4], breaking the trade-off between flexibility and the energy efficiency.

Since the birth of RHex, researchers have been trying to develop new generation prototypes to further improve its capabilities. Edubot was equipped with the spatial compliance of the tunable leg to improve its adaptability, efficiency and robustness [5]; Whegs adopted wheel-leg structure to negotiate obstacles and traverse irregular terrain [6]; furthermore, T-RHex enhanced the vertical mobility by using microspines [7]; in addition, the swappable propulsor robot could replace the RHex legs with other wearable equipment for a wide range of locomotion capability [8]. As a conclusion, most of new generation prototypes focus on overcoming extreme environments and improving their energy efficiency, however, research on the versatility and smooth stability is relatively rare.

In recent years, the transformable mechanisms have been widely studied. With the innovative transformable mechanical structures, the robots can switch between multiple mobile modes, thereby guaranteeing energy efficiency and flexibility in different environments, such as the retractable wheel-leg quadruped robot [9], Quattroped [10], the Claw-Wheel Transformable Robot [11]

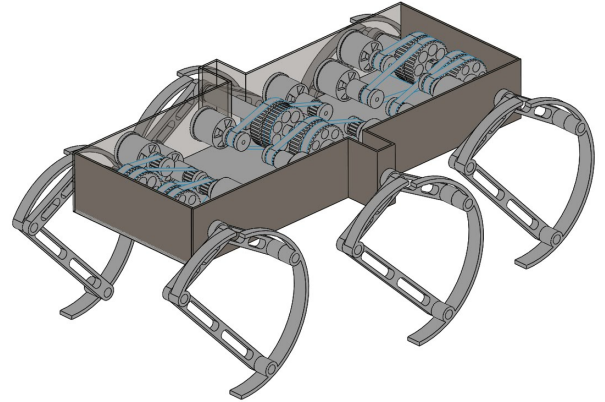


Fig. 1. Mechanical structure of RHex-T3

and TurboQuad [12]. Obviously, the transformable mechanism has great research potential.

Therefore, we designed RHex-T3 by replacing the roller legs of RHex to the innovative transformable mechanical structure. RHex-T3 not only inherits most of RHex's mobility, but also can switch to the RHex-mode, the wheel-mode and the leg-mode freely. Smooth locomotions can be generated through wheel-mode and leg-mode for further improving the energy efficiency and smooth mobility. In addition, the transformable mechanical structure derivatively enhances RHex-T3's versatility through the claw-mode to transport objects and the hook-mode to climb ladders. As the contribution of this paper, an innovative 2-DoF transformable mechanism based on the four-bar linkage was designed, which provides a new way to inherit and extend the capability of traditional high-performance robots.

## II. MECHANICAL DESIGN

### A. Overview

Fig. 1 illustrates the mechanical structure of RHex-T3, which consists of the trunk and 6 transformable legs. Each transformable leg has 2 DoF, and are separately driven by the two motors fixed in the trunk through the coaxial transmission.

The coaxial transmission mechanism inspired by Doggo [13] consists of the internal shaft and the external shaft, which respectively drive Rods 1 and 2 of transformable leg to rotate, as illustrated in Fig. 3. Besides, we further offset the two middle legs to avoid interference with the front and rear legs.

\*This work was supported by The Tianjin Science and Technology Program (19PTZWHZ00020) and Excellent Science and Technology Enterprise Specialist Project of Tianjin (No.18JCTPJC59000).

<sup>1</sup> is with the School of Computer science and Technology, Tiangong University, Tianjin, China xxiao@tiangong.edu.cn

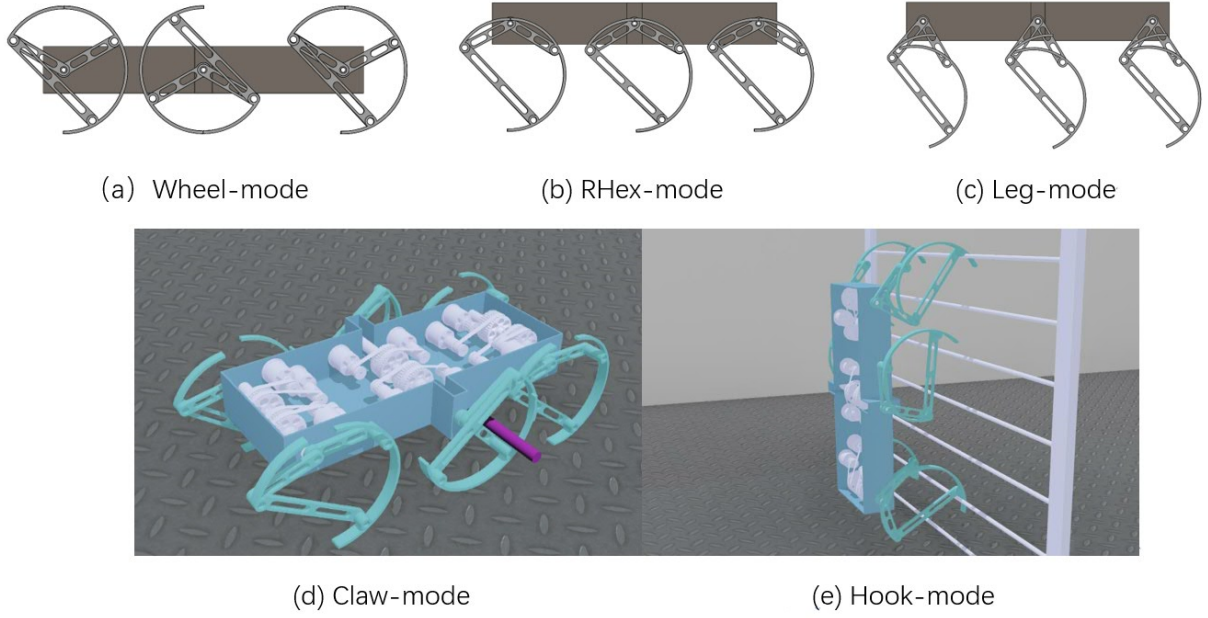


Fig. 2. 5 modes of RHex-T3

The transformable leg structure is designed based on the four-bar linkage mechanism, and consists of the Rods 1,2,3 and the Arc 1, as illustrated in Fig. 4. In addition, by designing the leg structure on different planes to maximize the workspace, the range of the angle  $\alpha$  between Rods 1 and 2 is varied from  $33.02^\circ$  to  $326.98^\circ$ ; if the relative angle between Rods 1 and 2 remains unchanged, the transformable leg can rotate around the motor shaft without restriction.

### B. Modes Generation

Fig. 2 illustrates the 5 modes of RHex-T3 for locomotion and operation.

The wheel-mode is illustrated in Fig. 2(a). When the motor shaft moves to the center of the Arc 1, the outer arcs of the transformable leg form a 2/3 circle. Then, the left and right tripods are synchronized with each other and are kept  $180^\circ$  out of phase with the opposite side. Hence the robot can roll forward when all the motors

rotate at the same speed.

When the motor shaft moves to the upper end of the Arc 1, the 2/3 circle is formed by outer arcs again, and the robot transforms to the RHex-mode, as illustrated in Fig. 2(b). When the relative angle between Rods 1 and 2 remains unchanged, the robot can rotate its legs without restriction. The RHex-mode inherits most of the mobility of RHex.

When the transformable leg is regarded as a four-bar linkage which is controlled by the coaxial motors, RHex-T3 switches to the leg-mode with great flexibility and smooth mobility, as illustrated in the Fig. 2(c). In the leg-mode, the robot can generate various walking gaits and overcome obstacles by controlling the landing point.

In addition, RHex-T3 can also switch to the claw-mode and the hook-mode to improve its versatility as illustrated in Figs. 2(d) and 2(e). Due to the complexity of these two modes, their transformation and capabilities

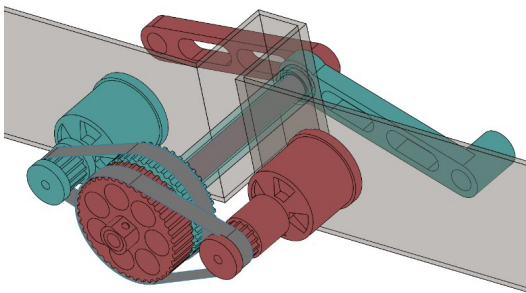


Fig. 3. Coaxial transmission mechanism

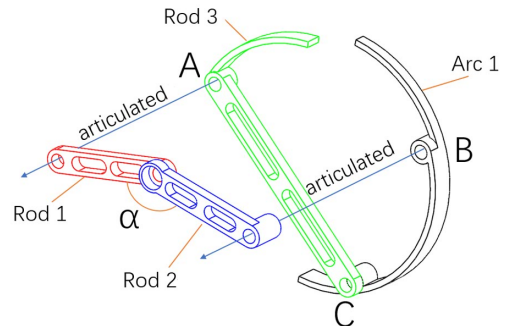


Fig. 4. Transformable leg structure

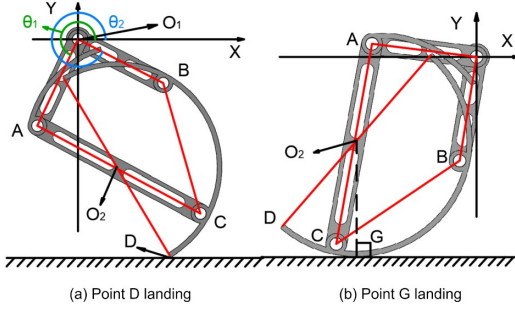


Fig. 5. The coordinates of the transformable leg

will be introduced in the simulation experiments in detail.

### III. KINEMATICS

#### A. Forward Kinematics

The mechanical structure of the transformable leg greatly enriches the capabilities of RHex-T3, however, it also increases the computational complexity of the kinematics. Therefore, the forward kinematics is elaborated in detail to analyze the workspace of the transformable leg.

Fig. 5 illustrates the Cartesian coordinate, of which the origin is set on the motor shaft as  $O_1$ , and the x-axis is horizontal to the body. Rods  $O_1A$  and  $O_1B$  are directly connected to the motor shaft  $O_1$ , and their lengths are set as  $O_1A = O_1B = r$ . Rod  $AC$  is linked to Rod  $O_1A$ . Arc  $\widehat{BCD}$  is a semicircle, of which the center is set as  $O_2$  and the radius is also equal to  $r$ . In addition,  $\angle DO_2C = \frac{\pi}{6}$  and  $\angle DO_2B = \frac{2\pi}{3}$ .  $\theta_1$  and  $\theta_2$  are separately set as the angles of Rod  $O_1A$  and Rod  $O_1B$  with respect to x-axis.

In the walking locomotion, there are two situations of landing. The first one is using Point D at the end of Arc 1, and the other one is using the tangent point of Arcs with the ground (Point G). Therefore, the coordinates of the landing point should be calculated separately in the forward kinematics. In addition, there are other positions that will play a role in special modes besides D, such as Points C, B and the other points on the arcs.

#### B. Inverse Kinematics

Since there are two different landing methods in the leg-mode, the calculation of the inverse kinematics should also be considered separately, which will not be derived in detail here. In general, the choice of landing method is based on the constraint of the workspace and the constraint of the velocity at the landing point.

### IV. SIMULATION PLATFORM AND CONTROL STRUCTURE

#### A. Simulation Platform

The simulation model of the RHex-T3 robot is conducted by Webots simulation platform. As an open source platform, Webots provides a complete development environment to model, program and simulate

TABLE I  
Simulation parameters of RHex-T3

|            |                  |                                 |                |       |
|------------|------------------|---------------------------------|----------------|-------|
| Body       | Length           | 550mm                           | Height         | 80mm  |
|            | Width            | 306mm                           |                |       |
| Legs       | Length of $O_1A$ | 100mm                           | Length of $AC$ | 193mm |
|            | Length of $O_1B$ | 100mm                           | $r$            | 100mm |
| Material   |                  | Aluminum                        |                |       |
| Density    |                  | $2.7 \times 10^3 \text{kg/m}^3$ |                |       |
| Total Mass |                  | 11.3294kg                       |                |       |

robots. By importing the model of the SolidWorks, the physical structure of the simulation model is exactly the same as the mechanical design. The mechanical parameters in the simulation are listed in TABLE I.

In addition, the parameters of the contact model and the Coulomb friction model are chosen as the system default values. In the simulation, the position of the motor shafts are simplified to locate at the connection of the legs. Therefore, the gears will not rotate in the simulations.

#### B. Mobile Control System

The mobile control system of RHex-T3 consists of the instruction layer, the planner layer and the behavior layer, as illustrated in Fig. 6.

The instruction layer only processes high-level instructions, such as the mobile mode, gait, speed, steering and other macro instructions. And then sends the control information to the corresponding mode controller to convert the speed into motion parameters such as angular velocity in wheel-mode, the gait, step length and step period in leg-mode, or the gait and angular velocity in RHex-mode. The control parameters will be sent to the planner layer.

The planner layer connects the instruction layer and the behavior layer. Therefore, it can translate the control parameters into the trajectory of CoM. Then, the controller generates the trajectory of the landing points based on the terrain information and the CoM trajectory. After that, the controller calculates the angle trajectory of the joints by the inverse kinematics. Finally, it sends the information to the behavior layer.

The behavior layer faces to the actuators. The behavior layer converts the desired angle position into the torque values by using a PID controller, and drives the actuators.

### V. SIMULATION RESULT

#### A. Locomotion

The simulations were conducted to verify RHex-T3's mobility in three mobile modes. In each mode, the alternating tripod gait was chosen to be analyzed, whereby the legs forming the left and right tripods were synchronized with each other and kept an opposite mobile-mode phase with the opposite tripod. To explore their respective gait properties, the torque and the

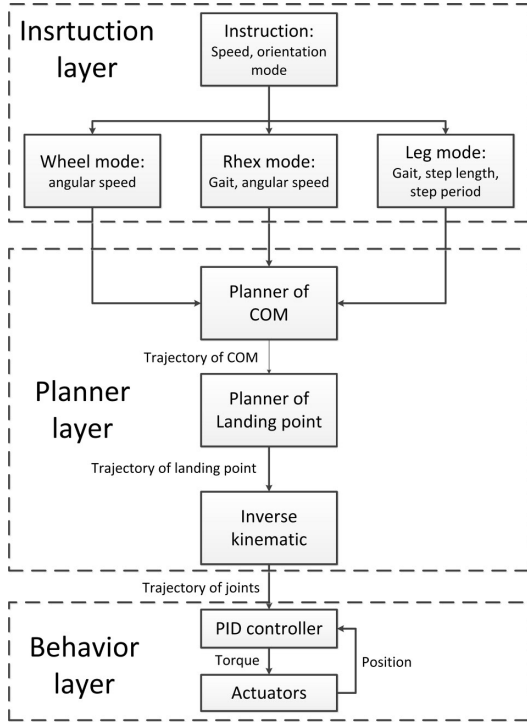


Fig. 6. Overall Control Structure

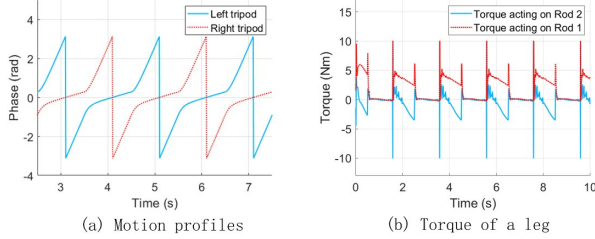


Fig. 7. Motion profiles and the torque for left and right tripods in RHex-mode when  $\phi_s = 40^\circ$  and  $T_c = 2s$

specific resistance of each mode were compared and analyzed.

#### (1) RHex-mode

In the RHex-mode, the robot moves the motor shaft to the upper end of Arc 1, and generates the alternating tripod gait. With reference to the control strategy of RHex [1], each period is divided into slow and fast swing phases, of which the corresponding speeds are controlled to ensure that each of them accounts for a half period. The control parameters are listed in Tables II. The simulations were conducted and the motion profiles and the torque for left and right tripods at speed of 0.2m/s were illustrated in Fig. 7.

#### (2) Wheel-mode

In the wheel-mode, the motor shaft is moved to the center of Arc 1, and then the alternating tripod gait is generated to make up for the vacancy of the opposite arc, ensuring the CoM moves forward steadily. The angular velocity of all the coaxial motors is the control parameter. Various simulations at different speeds were conducted.

#### (3) Leg-mode

In the leg-mode, there are two phases during each step, the swing phase and the stance phase. The alternating tripod gait is generated by switching between the supporting tripod and the swinging tripod, which makes the robot can easily overcome obstacles by adjusting the landing point during the swing phase. The control parameters were listed in Tables II, and thus the simulations at various speeds were conducted by adjusting the step length and the step time. The time of the swing phase (swing up phase and swing down phase) is equal to the time of the stance phase, which means Duty factor=50%. The torque of the left front leg when step length=0.16m and step period=1.6s is illustrated in Fig. 9.

For each gait/mode, the energy consumption condition was evaluated by using an index called specific resistance (SR) [14], which is determined by the gravity of the robot ( $mg$ ), its averaged power consumption ( $P$ ), and its averaged forward speed ( $v$ ) as follows.

$$SR = \frac{P}{mgv} \quad (1)$$

Fig. 10 illustrated SR in each mode at different velocities. Obviously, the wheel-mode had the best performance because of its high energy efficiency. When the speed increased in the wheel-mode, SR could still maintain a low value. The RHex-mode had similar SR values with the leg-mode. The tripods gait in the leg-mode was helpful to improve the energy efficiency, but limited the walking speed. In addition, RHex-mode could generate a very fast speed, however, the energy loss during the collisions affected its energy efficiency.

#### B. Target Object Transportation

RHex-T3 not only inherits most of RHex's mobility, but also can grasp and transport some objects by the claw-mode. In detail, by performing the middle legs as two claws, RHex-T3 converts to a quadruped robot for grasping and transporting. In the simulations, the states of the objects are assumed to be known. The process of transporting can be divided into 4 steps as follows.

Step 1: RHex-T3 moves to the center position of the captured object. The middle two legs are flipped over and transform into two claws, and now the robot is supported

TABLE II  
Control parameters of each mode

| Mode  | Control parameters                 |                 |
|-------|------------------------------------|-----------------|
| RHex  | Leg sweep angle for slow leg swing | $\phi_s$        |
|       | Leg sweep angle for fast leg swing | $2\pi - \phi_s$ |
|       | Step period of RHex-mode           | $T_c$           |
| Wheel | Angular velocity                   | $V_w$           |
| Leg   | Step length                        | $L_s$           |
|       | Step period                        | $T_s$           |
|       | Maximum leg lift height            | $h_m$           |
|       | Duty factor                        | 50%             |



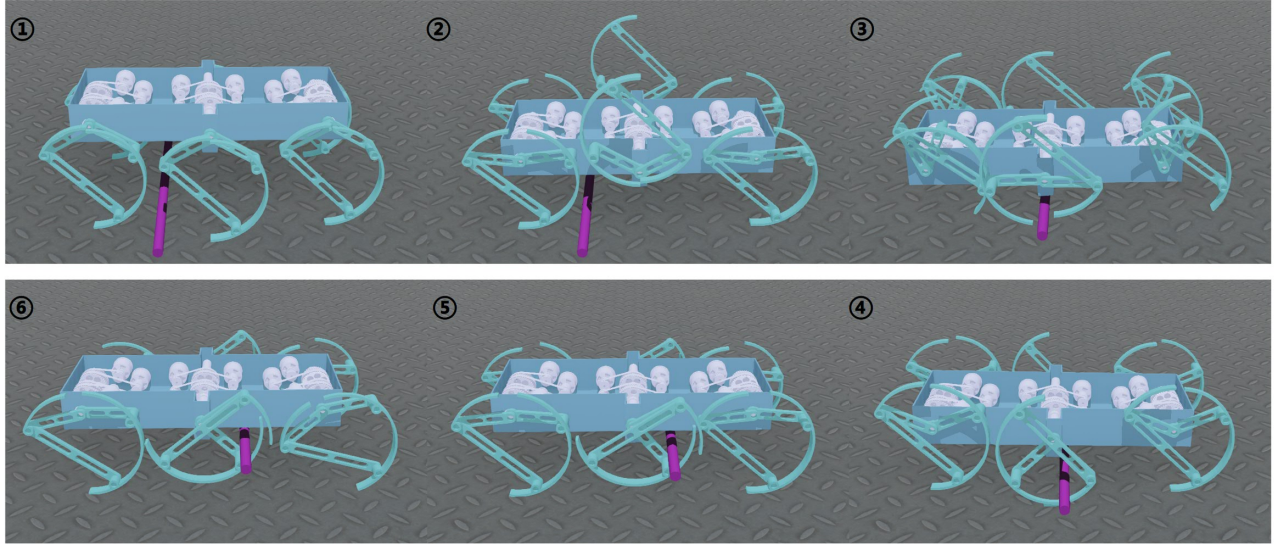


Fig. 8. The sequential motions of transportation

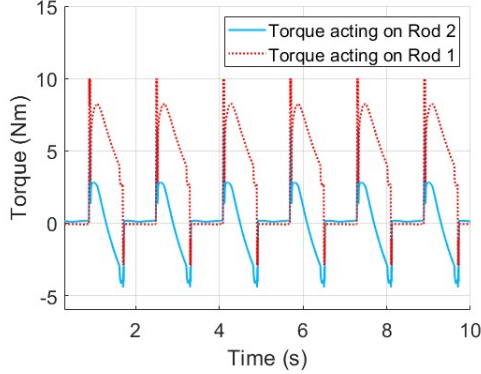


Fig. 9. The torque of the left front leg in leg-mode when step length=0.16m and step period=1.6s

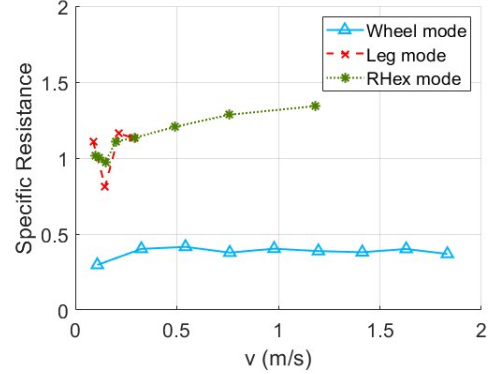


Fig. 10. SR in each mode at different velocities

by the front and rear legs. The controller thus plans the motion trajectory of grasping.

Step 2: The supporting legs then adjust the height of the robot according to the grasping trajectory, and then the claws tighten up to grasp the object.

Step 3: Revolve the motors to press the objects close the body so that the object will not shift or fall during the transportation.

Step 4: RHex-T3 evaluates the weight of the transported object according to the torque of the claw, and thus plans the gait trajectory to keep the CoM around the intersection of the diagonals of the supporting legs. As a result, walking or trot gaits are generated through the supporting legs for the transportation missions.

The simulations were conducted to verify the transport capacity of RHex-T3 by using a cylinder with a length of 1m of 2.7kg. Fig. 8 illustrated the sequential motions.

As a conclusion, the capability of grasping is affected by the shape of the target objects. RHex-T3 is good at

grasping some thin and long objects of uniform quality with the maximum mass of 2.7kg, but its load capacity is much higher than that. The transport capability of RHex-T3 still needs to be further explored in future work.

### C. Climb Ladders

In previous research of RHex, the capability of climbing stairs has been fully developed [15], however, climbing ladders is still a great challenge. In this paper, by switching to the hook-mode to imitate the praying mantis, RHex-T3 successfully climbed the ladders in the simulations. Two ladders were built in the simulations, one of which is perpendicular to the ground, and the other is at  $45^\circ$  to the ground. The specific parameters of the ladders are listed in the TABLE III.

Similar to the walking gait of quadruped robots, the strategy of climbing ladders is that RHex-T3 stays in a statically stable state during the motion. In detail, when the middle and rear legs are controlled to hook

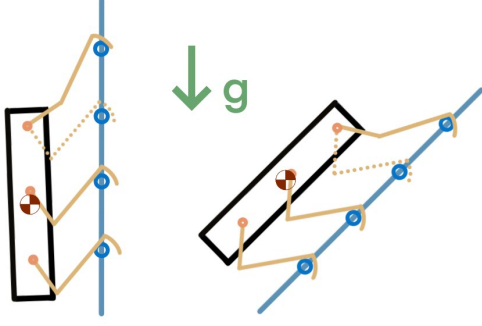


Fig. 11. The strategy of climbing ladders

the ladder, RHex-T3 can stay in a statically stable state even if the front legs leave the lattice, and thus the front legs can move to the next lattice according to the inverse kinematics and hook it, as illustrated in Fig. 11. The process of climbing ladders can be divided into 5 steps as follows.

Step1: Adjust the initial posture of the robot on the ladder so that its six legs can be firmly hooked on the ladder.

Step2: Fix the middle and rear legs to hook on the ladder, and then move the front legs to leave the current lattice without being interfered by the ladder.

Step3: Further control the front legs to hook the next lattice without collision.

Step4: Control the middle and rear legs sequentially to leave the current lattice and hook the next lattice with reference to Steps 2 and 3.

Step5: Return all legs back to the initial posture to move the robot forward along the ladder, and then go back to step 1 to repeat the cyclic process until reaching the top of the ladder.

As the simulation result, Fig. 12 illustrated the sequential motions of climbing a 90° ladder and Fig. 13 illustrated the torque of the front left leg during the climb motion. The front leg left the ladder at 0.8s and hooked the next lattice at 1.1s. At 5.9s the robot moved upward and then began a new cycle process at 6.7s.

Similarly, the simulation of climbing the 45° ladder was also conducted successfully. Please refer to the attached video for the detailed process. As a conclusion, RHex-T3's capability of climbing ladders is undoubtedly excellent.

TABLE III  
Parameters of ladders

| Angle of Ladder           |               | 90°      | 45° |
|---------------------------|---------------|----------|-----|
| Lattice                   | Shape         | Cylinder |     |
|                           | Bottom Radius | 0.01m    |     |
|                           | Length        | 1m       |     |
| Distance between lattices |               | 0.12m    |     |

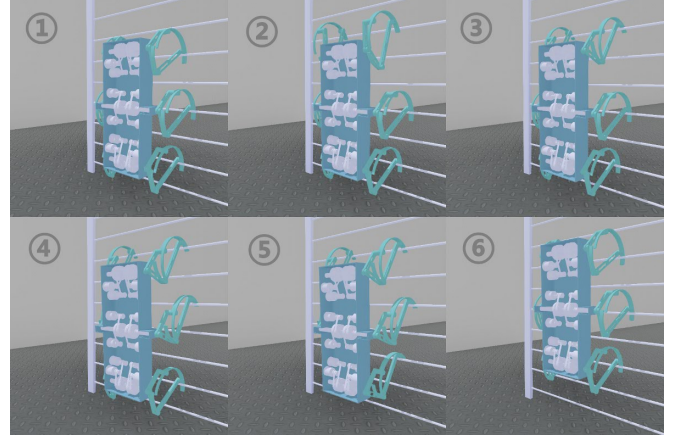


Fig. 12. The sequential motions when climbing the 90° ladder

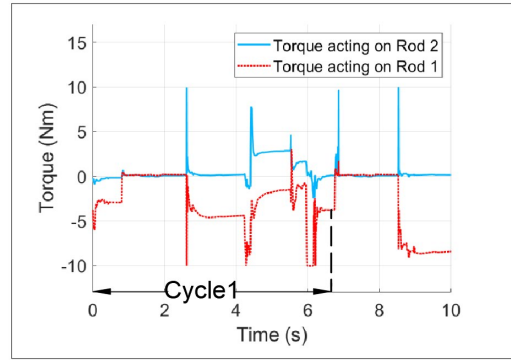


Fig. 13. Torque of the front leg when climbing the 90° ladder

## VI. CONCLUSION AND FUTURE WORK

In this paper, RHex-T3 inspired by RHex was developed by using the novel transformable mechanism. The mechanism design of RHex-T3 and its 5 transformable modes were introduced, and the kinematics of the transformable leg was discussed and calculated in detail. Then the simulation model of RHex-T3 was conducted based on its mechanical structure. The properties of locomotion in each mobile mode were analyzed and compared. In addition, the functions of grasping, transporting and climbing ladders were also verified through the simulations.

As the future work, the prototype of RHex-T3 will be built. The mobility inherited from RHex will be tested, and the functions of other modes will be verified through physical experiments. RHex-T3 still has huge potential to be discovered in terms of flexibility and versatility.

## References

- [1] U. Saranli, M. Buehler, D.E. Koditschek, "RHex: A Simple and Highly Mobile Hexapod Robot," *Int. J. of Robotics Research*, Vol. 20, No. 7, pp. 616–631, 2001.
- [2] R. Altendorfer, N. Moore, H. Komsuoglu, M. Buehler, H. B. Brown Jr., D. McMordie, U. Saranli, R. J. Full, and D. E. Koditschek, "RHex: A biologically inspired hexapod runner," *Autonomous Robots*, Vol. 11, No. 3, pp. 207–213, 2001.

- [3] U. Saranli, W. J. Schwind and D. E. Koditschek, "Toward the control of a multi-jointed, monopod runner," *Proceedings IEEE International Conference on Robotics and Automation*, pp. 2676–2682, 1998.
- [4] D. McMordie, C. Prahacs and M. Buehler, "Towards a dynamic actuator model for a hexapod robot," *IEEE International Conference on Robotics and Automation*, pp. 1386–1390, 2003.
- [5] K. C. Galloway, E. C. Jonathan, and D. E. Koditschek, "Design of a Multi-Directional Variable Stiffness Leg for Dynamic Running," *Proceedings of the ASME 2007 International Mechanical Engineering Congress and Exposition*, pp. 73–80, 2007.
- [6] P. A. Dunker, W. A. Lewinger, A. J. Hunt and R. D. Quinn, "A biologically inspired robot for lunar In-Situ Resource Utilization," *IEEE/RSJ International Conference on Intelligent Robots and Systems*, pp. 5039–5044, 2009.
- [7] M. Martone, C. Pavlov, A. Zeloof, V. Bahl, and A. M. Johnson, "Enhancing the Vertical Mobility of a Robot Hexapod Using Microspines," *arXiv e-prints*, 2019.
- [8] R. Kim, A. Debate, S. Balakirsky, and A. Mazumdar, "Using Manipulation to Enable Adaptive Ground Mobility " *IEEE International Conference on Robotics and Automation*, pp. 857–863, 2020.
- [9] K. Tadakuma, R. Tadakuma, A. Maruyama, E. Rohmer, K. Nagatani, K. Yoshida, A. Ming, S. Makoto, M. Higashimori, and M. Kaneko, "Armadillo-Inspired wheel-leg retractable module," *IEEE International Conference on Robotics and Biomimetics*, pp. 610–615, 2009.
- [10] S. Shen, C. Li, C. Cheng, J. Lu, S. Wang and P. Lin, "Design of a leg-wheel hybrid mobile platform," *IEEE/RSJ International Conference on Intelligent Robots and Systems*, pp. 4682–4687, 2009.
- [11] J. Chou and L. Yang, "Innovative design of a claw-wheel transformable robot," *IEEE International Conference on Robotics and Automation*, pp. 1337–1342, 2013.
- [12] W. Chen, H. Lin, Y. Lin and P. Lin, "TurboQuad: A Novel Leg-Wheel Transformable Robot With Smooth and Fast Behavioral Transitions," *IEEE Transactions on Robotics*, Vol. 33, No. 5, pp. 1025–1040, 2017.
- [13] N. Kau, A. Schultz, N. Ferrante and P. Slade, "Stanford Doggo: An Open-Source, Quasi-Direct-Drive Quadruped," *2019 International Conference on Robotics and Automation*, pp. 6309–6315, 2019.
- [14] G. Gabrielli and T. H. von Karman, "What price speed? " *ASME Mech*, Vol. 72, No. 10, pp. 775–781, 1950.
- [15] E. Z. Moore and M. Buehler, "Stable Stair Climbing in a Simple Hexapod," In *Proceedings of the 4th Int. Conf. on Climbing and Walking Robots*, pp. 603–610, 2001.